Molecular Therapy
Nucleic Acids
Original Article

MicroRNA let-7i Inhibits Histone Lysine Demethylase KDM5B to Halt Esophageal Cancer Progression

Yang Yang,[1,3] Wenhua Li,[1,3] Bochong Wei,[1,3] Kai Wu,[1] Donglei Liu,[1] Dengyan Zhu,[1] Chunyang Zhang,[1] Fengbiao Wen,[1] Yuxia Fan,[2] and Song Zhao[1]

[1]Department of Thoracic Surgery, The First Affiliated Hospital of Zhengzhou University, Zhengzhou 450015, P.R. China; [2]Department of Thyroid Surgery, The First Affiliated Hospital of Zhengzhou University, Zhengzhou 450015, P.R. China

Recent studies have suggested that microRNA let-7i is a tumor suppressor in human cancers, including esophageal cancer, but its underlying mechanism is not yet fully understood. We investigated the role and mechanisms of let-7i in the progression of esophageal cancer. We first showed that let-7i was downregulated in esophageal cancer tissues and cells and then linked its low expression to cancer progression. Bioinformatic analysis predicted KDM5B as a target gene of let-7i, which was confirmed by a dual-luciferase reporter assay. Loss- and gain-of function approaches were adopted to examine the interactions of let-7i, KDM5B, SOX17, and GREB1 *in vitro* and *in vivo*. Overexpression of let-7i suppressed esophageal cancer cell proliferation and invasion and promoted apoptosis. Mechanistic investigation showed that let-7i targeted and inhibited KDM5B expression, whereas KDM5B enhanced H3K4me3 at the SOX17 promoter region. Overexpression of let-7i suppressed the expression of GREB1 in esophageal cancer cells by regulating the KDM5B/SOX17 axis *in vivo* and *in vitro*. Taken together, our findings reveal the tumor-suppressive properties of let-7i in esophageal cancer in association with an apparent KDM5B-dependent SOX17/GREB1 axis. This study offers a potential prognostic marker and therapeutic target for esophageal cancer.

INTRODUCTION

Esophageal cancer, the eighth most common form of malignancy, is the sixth most common cause of cancer-related death in the world.[1] According to the most recent clinical study, the 5-year survival rate of patients with esophageal cancer is less than 20%, plummeting to less than 1% in patients with advanced esophageal cancer.[1] This state of affairs calls for improved early diagnostic and treatment strategies. This unmet need motivated us to focus on the basic molecular aspects of the pathogenesis of esophageal cancer. An increasing body of evidence has revealed the critical roles of microRNAs (miRNAs) in human diseases, including cancer.[2–4] The miRNAs exert either promotive or suppressive effects on tumorigenesis. For instance, miR-556-3p has been demonstrated to facilitate esophageal cancer progression,[5] whereas miR-145 impairs the metastasis of upper tract urothelial carcinoma.[6] In addition, aberrant expression of miRNAs in human cancer is often a marker of carcinogenesis.[7] For example, downregulation of let-7 family members has been observed in multiple human cancers, such as esophageal, lung, and breast cancers.[8–10] These findings have highlighted the tumor-suppressive role of let-7 family members. Importantly, let-7i possesses inhibitory effects on the development of a variety of cancers, including lung cancer and bladder cancer.[11,12] However, the role of let-7i in esophageal cancer remains to be clarified.

Accumulating evidence has revealed that histone lysine demethylase 5b (KDM5B) functions as an oncogene, which facilitates cancer cell proliferation, migration, and survival in multiple types of human cancer, including esophageal cancer.[13] Moreover, as a master regulator of the methylome at lysine 4 of histone 3 (H3K4), KDM5B has been shown to exert suppressive effects on expression of tumor suppressor genes by increasing the level of try-methylation of H3K4 (H3K4me3) at the promoter region of those genes.[14] For instance, upregulation of KDM5B resulted in downregulation of caveolin-1, a tumor suppressor, in breast cancer.[15] Moreover, elevated KDM5B has been related with increased expression of E2F transcription factors,[16] which have been shown to be upregulated in a variety of human cancers, hence, serving as a prognostic marker of tumorigenesis.[16,17] Interestingly, a previous study has indicated that KDM5B promotes the progression of breast cancer through epigenetic repression of let-7.[18] However, the involvement of let-7 and KDM5B in the pathogenesis of esophageal cancer remains to be elucidated.

Received 19 May 2020; accepted 11 September 2020;
https://doi.org/10.1016/j.omtn.2020.09.012.

[3]These authors contributed equally to this work.

Correspondence: Yuxia Fan, Department of Thyroid Surgery, The First Affiliated Hospital of Zhengzhou University, No. 1, Eastern Jianshe Road, Zhengzhou 450015, Henan Province, P.R. China.
E-mail: fccfanyx@zzu.edu.cn
Correspondence: Song Zhao, Department of Thoracic Surgery, The First Affiliated Hospital of Zhengzhou University, No. 1, Eastern Jianshe Road, Zhengzhou 450015, Henan Province, P.R. China.
E-mail: zhaosong@zzu.edu.cn

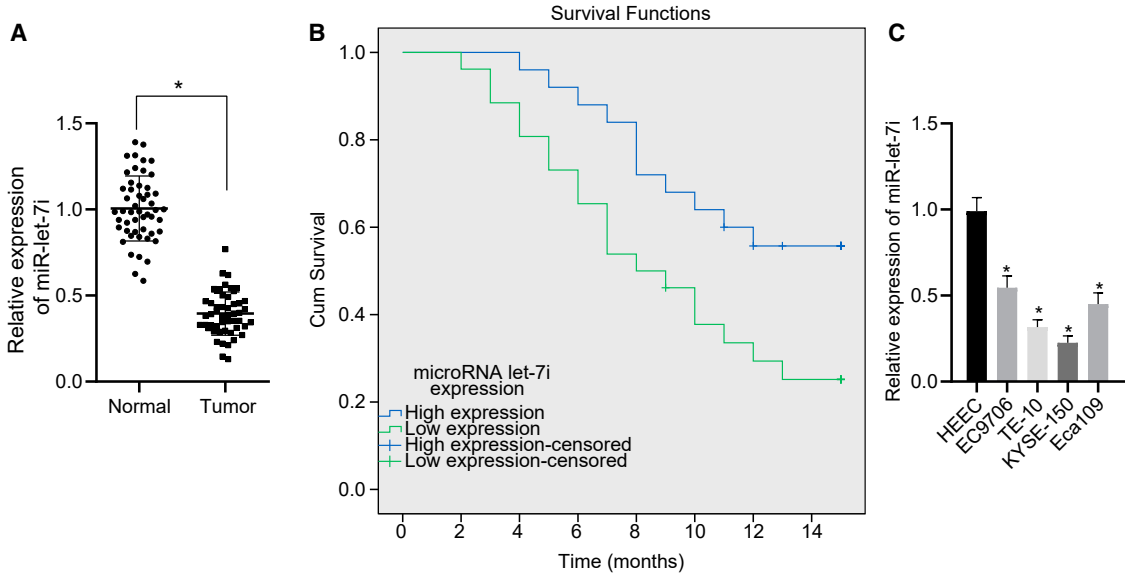

Figure 1. MicroRNA let-7i Is Downregulated in Esophageal Cancer

(A) Result of qRT-PCR determining let-7i expression in esophageal tumors (n = 51). *Tumor group versus normal group, $p < 0.05$. (B) Overall survival time of patients with esophageal cancer with relatively high let-7i expression and those with low let-7i expression as analyzed by the Kaplan-Meier method. (C) Results of qRT-PCR determining the expression of let-7i in esophageal cancer cells (EC9076, Eca109, KYSE-150, and TE-10) and normal esophageal epithelial cells (HEEC). *$p < 0.05$ versus HEEC.

In this study, we explored the role of let-7i in esophageal cancer progression *in vitro* and *in vivo* and identified a mechanism by which let-7i mediates that progression. We report a series of experiments showing that let-7i impairs the development of esophageal cancer by inhibiting the expression of KDM5B in an SRY-box 17 (SOX17)/gene regulated in breast cancer 1 (GREB1)-dependent manner. Our study has furthered our knowledge about let-7i in the pathogenesis of esophageal cancer and identifies novel potential therapeutic targets for this malignancy.

RESULTS

Downregulation of let-7i in Esophageal Cancer Is of Clinicopathological Significance

An increasing body of evidence has revealed the critical roles of let-7i in the progression of multiple types of cancers, including myeloma, hepatoblastoma, and esophageal cancer.[19–21] Therefore, to investigate whether let-7i was indeed associated with the clinicopathological features of esophageal cancer, we determined its expression level in esophageal tumor tissues and paired it with adjacent healthy tissues (n = 51). The results showed significantly lower expression of let-7i in tumors than that in adjacent healthy tissues (Figure 1A). In addition, the correlation analyses between let-7i expression and clinicopathological features showed close correlations between low let-7i expression and large tumor size; advanced tumor, node, and metastasis (TNM) stage; and the presence of lymph node metastasis (LNM), irrespective of patient age and gender (Table 1). Using the median of the let-7i expression in the 51 patients with esophageal cancer as a cutoff point, we separated the patients into low and high let-7i expression groups. Kaplan-Meier evaluation of overall survival of the patients with esophageal cancer showed that patients with low let-7i expression had shorter survival times than did those with high let-7i expression (Figure 1B; $p < 0.05$). We also determined that the expression of let-7i in esophageal cancer cells (EC9076, Eca109, KYSE-150, and TE-10) and human esophageal epithelial cell line (HEEC) using quantitative reverse transcription-polymerase chain reaction (qRT-PCR). The results showed that the expression of let-7i was reduced in esophageal cancer cells; among which, KYSE-150 and TE-10 had the lowest expression of let-7i (Figure 1C). Thus, KYSE-150 and TE-10 were selected for further studies.

Overexpression of let-7i Inhibits Esophageal Cancer Cell Growth and Invasion and Promotes Cancer Cell Apoptosis

To investigate the role of let-7i in esophageal cancer progression, we altered its expression in KYSE-150 and TE-10 cells by transfection with a let-7i mimic or a mimic negative control (NC) and then confirmed the enforced expression after let-7i mimic transfection by qRT-PCR (Figure 2A). We next investigated whether let-7i was associated with esophageal cancer cell proliferation by using the 5-ethynyl-2′-deoxyuridine (EdU) assay, which showed that let-7i overexpression inhibited cancer cell proliferation ($p < 0.05$) (Figure 2B). Moreover, the metastatic potency of esophageal cancer cells was evaluated by transwell invasion assay *in vitro*, which showed that cells transfected with the let-7i mimic displayed reduced invasive ability (Figure 2C). Furthermore, the effect of let-7i on esophageal cancer cell apoptosis was also evaluated by flow cytometry, which showed that overexpressing let-7i facilitated cellular apoptosis in esophageal cancer cells (Figure 2D). Hence, let-7i overexpression could prevent the progression of esophageal cancer *in vitro*.

Table 1. Relationships between let-7i Expression and Esophageal Cancer Pathophysiological Features

Clinical Features	Case Number	let-7i Expression	p Value
Age (y)			0.723
<65	31	0.390 ± 0.114	
≥65	20	0.403 ± 0.145	
Gender			0.582
Male	30	0.387 ± 0.104	
Female	21	0.407 ± 0.154	
Tumor Size (cm)			0.009
<5	35	0.426 ± 0.121	
≥5	16	0.328 ± 0.113	
TNM Staging			0.008
I	21	0.442 ± 0.133	
II	16	0.403 ± 0.113	
III	14	0.317 ± 0.094	
LNM			0.017
Negative	24	0.439 ± 0.126	
Positive	27	0.356 ± 0.114	

Note: TNM, tumor, node, metastasis; LNM, lymph node metastasis.

let-7i Targets KDM5B in Esophageal Cancer

To understand how let-7i exerts its inhibitory effects on esophageal cancer progression, we analyzed the downstream molecular events provoked by let-7i. First, we predicted the potential target(s) of let-7i via online tools (starBase, mirDIP, and RAID) and obtained intersections of predicted genes. The gene intersection visualized using a Venn diagram suggested that KDM5B may be a critical target controlled by let-7i (Figure 3A). Importantly, the expression of KDM5B has been shown previously to be upregulated in esophageal cancers,[13] which was in alignment with the result obtained from starBase database (Figure 3B). To further validate this finding, we detected the expression of KDM5B in esophageal tumors using immunohistochemistry and immunoblotting analyses. This showed that the expression of KDM5B was elevated in esophageal tumors (Figures 3C and 3D). Meanwhile, results from western blot analysis of KDM5B protein levels in esophageal cancer cells and HEEC revealed that KDM5B was upregulated in esophageal cancer cells (Figure 3E). Given the reduced expression of let-7i in esophageal tumors, it was reasonable to postulate that let-7i could target KDM5B to suppress its expression. We investigated that possibility by performing dual-luciferase reporter assays to evaluate the relationship between let-7i and KDM5B, using the predicted binding sequence obtained from starBase (Figure 3F). The results showed that cells co-transfected with let-7i mimic and reporter plasmid containing wild-type KDM5B 3′ UTR displayed reduced luciferase activity (Figure 3G). However, the luciferase activity was unaffected by co-transfection of let-7i and reporter vector cloned with KDM5B 3′ UTR containing a mutated binding sequence (Figure 3G). This finding confirmed that let-7i could target KDM5B in esophageal cancer cells. Then, we further evaluated the effect of let-7i on KDM5B expression at the protein level. First, we altered the expression of let-7i in esophageal cancer cells by transfection with let-7i mimic or let-7i inhibitor and validated the transfection efficiency by qRT-PCR (Figure 3H). Next, we determined the KDM5B protein level in those cells, finding that let-7i overexpression reduced KDM5B expression, whereas let-7i inhibitor transfection elevated KDM5B expression in esophageal cancer cells (Figure 3I). Taken together, our data demonstrated that let-7i could target KDM5B and suppress its expression in esophageal cancer.

let-7i Suppresses Esophageal Cancer Cell Growth and Migration While Promoting Their Apoptosis by Targeting KDM5B

Our data demonstrated that let-7i suppressed esophageal cancer progression, and let-7i targeted KDM5B in esophageal cancer cells. We then investigated whether let-7i mediated esophageal cancer suppression was KDM5B dependent. For that purpose, the expression of KDM5B and/or let-7i was overexpressed in KYSE-150 and TE-10 cells, and monitored by qRT-PCR (Figure 4A) and western blot analysis (Figure 4B), respectively. The results showed that the expression of let-7i was increased whereas that of KDM5B was decreased in response to let-7i mimic transfection; however, the expression of let-7i was not affected, whereas that of KDM5B was elevated by KDM5B overexpression plasmid (oe-KDM5B) in the presence of the let-7i mimic. Then, we investigated cell proliferation, invasion, and apoptosis using those transfected cells. The result of the EdU proliferation assay showed that let-7i overexpression inhibited esophageal cancer cell growth as reflected by a reduced cellular proliferation rate. However, let-7i failed to suppress cell proliferation in KDM5B-overexpressing esophageal cancer cells (Figure 4C). These findings indicated that the regulation of esophageal cancer cell growth by let-7i was dependent on KDM5B. Moreover, the result of the transwell invasion assay confirmed that cells transfected with let-7i displayed reduced invasion potency. However, upregulation of KDM5B compromised the inhibitory effects of let-7i overexpression on esophageal cancer cell invasion (Figure 4D). We further performed flow cytometry to detect cell apoptosis, finding that let-7i-mimic transfection significantly increased cell apoptosis, whereas that effect was diminished by KDM5B overexpression (Figure 4E). Together, these observations suggested that let-7i acted to inhibit esophageal cancer progression *in vitro* by targeting KDM5B.

KDM5B Silencing Promoted H3K4me3 and Enhanced the Expression of SOX17

KDM5B-related genes in esophageal cancer were predicted using LinkedOmics, which identified 8563 gene candidates (Figure 5A). We then analyzed the differentially expressed genes (DEGs) in esophageal cancer using datasets obtained from the GEO database (GenBank: GSE45168, GSE45670, and GSE100942), which uncovered 3,068, 2,978, and 699 DEGs, respectively (Figure 5B). After that, we obtained 318 human transcription factors from Cistrome and intersected them with the DEGs obtained from the GEO datasets. The Venn diagram results indicated 6 overlapped genes (Figure 5C). Among these candidates, SOX17 has been reported to be one of the downstream genes of KDM5B and is, furthermore, suppressed by

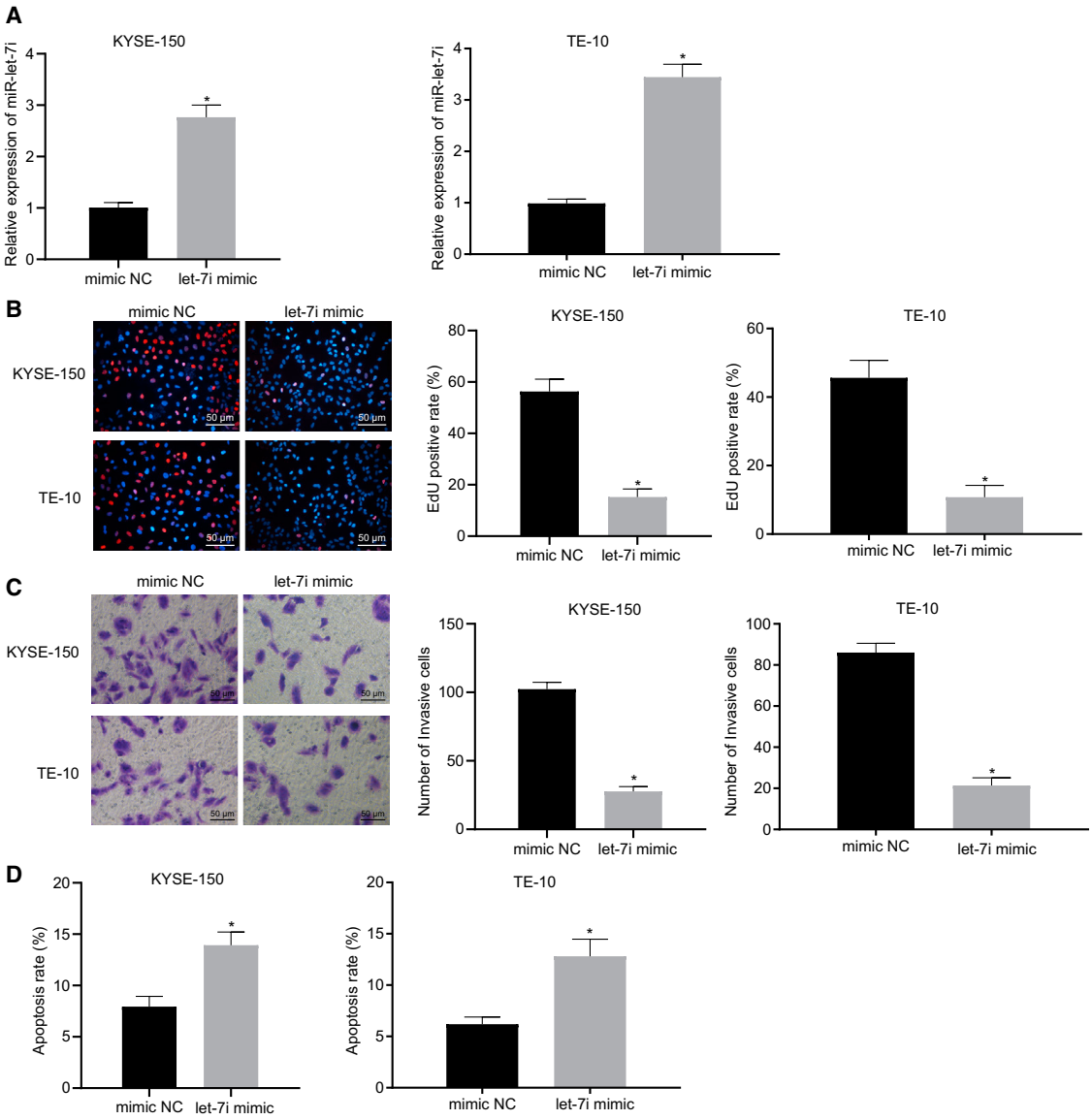

Figure 2. Upregulation of let-7i Inhibits Esophageal Cancer Cell Proliferation and Facilitates Cancer Cell Apoptosis

(A) Result of qRT-PCR evaluating the overexpression of let-7i in KYSE-150 and TE-10 cells. (B) Representative images and analyzed results of the EdU proliferation assay assessing the proliferation of KYSE-150 and TE-10 cells with or without let-7i overexpression. (C) Representative images and analyzed results of the transwell assay evaluating the cell invasion of KYSE-150 and TE-10 cells with or without let-7i overexpression. (D) Result of the flow cytometry determining the cell apoptosis of KYSE-150 and TE-10 cells under indicated conditions. *p < 0.05 versus mimic NC group.

KDM5B.[22] Meanwhile, the results of the Gene Expression Profiling Interactive Analysis (GEPIA) database showed downregulated expression of SOX17 in esophageal cancer (Figure 5D). Moreover, previous evidence has also suggested that SOX17 impairs the initiation of esophageal cancer.[23] Therefore, we speculated that KDM5B might promote the progression of esophageal cancer in a SOX17-dependent manner. To test that conjecture, we analyzed the relationship between the expression of SOX17 and KDM5B in esophageal cancer using the LinkedOmics database, which indicated that the expression of KDM5B was negatively correlated with that of SOX17 in esophageal cancer (Figure 5E). We then determined the expression of SOX17 in esophageal tumors and adjacent healthy tissues by western blot analysis, finding that SOX17 was significantly downregulated in tumor tissues (Figure 5F). Consistent with that result, the expression of SOX17 was also lower in esophageal cancer cells (EC9706, Eca109, KYSE-150, and TE-10) than it was in HEEC (Figure 5G). Having demonstrated the upregulation of KDM5B in esophageal cancer, it was reasonable to speculate that downregulation of SOX17 should be mediated by KDM5B. To test that hypothesis, we silenced the expression of KDM5B in esophageal cancer cells using short

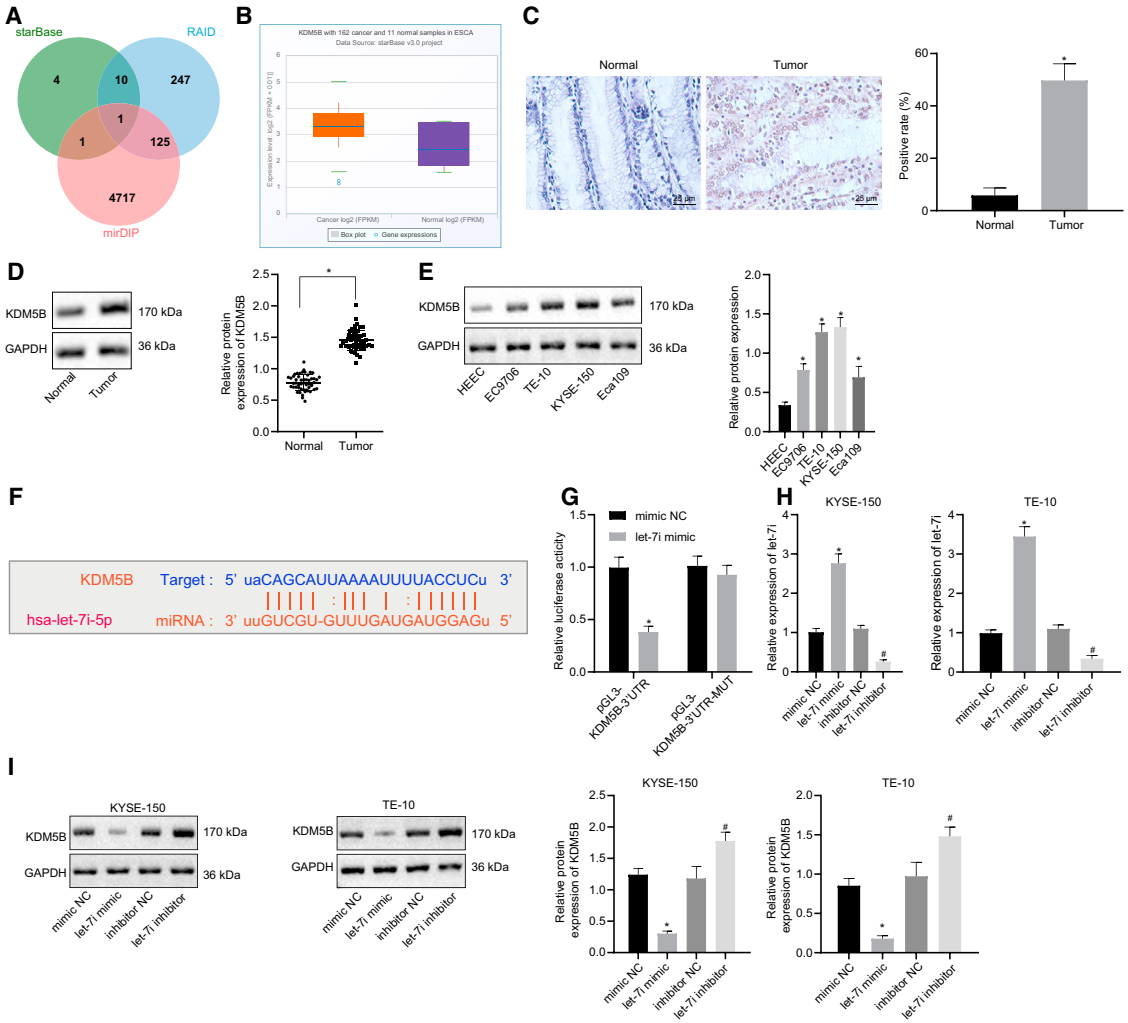

Figure 3. let-7i Targets KDM5B and Suppresses Its Expression in Esophageal Cancer

(A) Venn diagram displaying the predicted let-7i target genes obtained from online databases (starBase, mirDIP, and RAID), where KDM5B was at the intersection. (B) Results analyzed by starBase show the expression pattern of KDM5B in esophageal cancer samples and normal samples. (C and D) Results of immunohistochemistry analysis (C) and immunoblotting analysis (D) evaluating the expression of KDM5B in esophageal tumor tissue and paired normal tissues (n = 51). (E) Results of the western blot analysis measuring the expression of KDM5B in esophageal cancer cells and normal esophageal epithelial cells. (F) Binding sequence of let-7i in KDM5B 3′ UTR predicted by starBase. (G) Results of the dual-luciferase reporter assay evaluating the binding relationship between let-7i and KDM5B. (H) Results of the qRT-PCR determining the expression of let-7i in KYSE-150 and TE-10 cells under the indicated conditions. (I) Results of the western blot analysis measuring KDM5B protein levels in KYSE-150 and TE-10 cells under the indicated conditions. *$p < 0.05$ versus normal group or mimic NC group; #$p < 0.05$ versus inhibitor NC group.

hairpin RNA (shRNA) targeting KDM5B (sh-KDM5B) and validated the silencing efficiency via western blot analysis (Figure 5H). Upon determining the expression of SOX17 in those cells, we noticed that, compared with cells transfected with sh-NC, the expression of SOX17 was significantly increased in KDM5B-deficient cells (Figure 5I). We then evaluated H3K4me3 at the promoter region of SOX17 via chromatin immunoprecipitation (ChIP) assay, which showed that KDM5B silencing increased H3K4me3 enrichment at the SOX17 promoter region (Figure 5J). Taken together, these findings suggested that KDM5B knockdown could promote expression of SOX17 by promoting H3K4me3 at its promoter region.

KDM5B Knockdown Suppressed Esophageal Cancer Cell Proliferation and Invasion via Enhancing SOX17

To investigate further the roles of KDM5B and SOX17 in esophageal cancer, we depleted KDM5B and/or SOX17 in KYSE-150 and TY-10 cells and analyzed the altered expression of KDM5B and SOX17 in the cells by western blot analysis (Figure 6A). We then evaluated whether KDM5B mediated esophageal cancer progression by suppressing SOX17. First, we performed an EdU assay, which showed that KDM5B knockdown impaired cancer cell proliferation, whereas that suppressive effect was compromised by SOX17 silencing (Figure 6B). Moreover, cell invasion was evaluated by a transwell invasion assay, which revealed

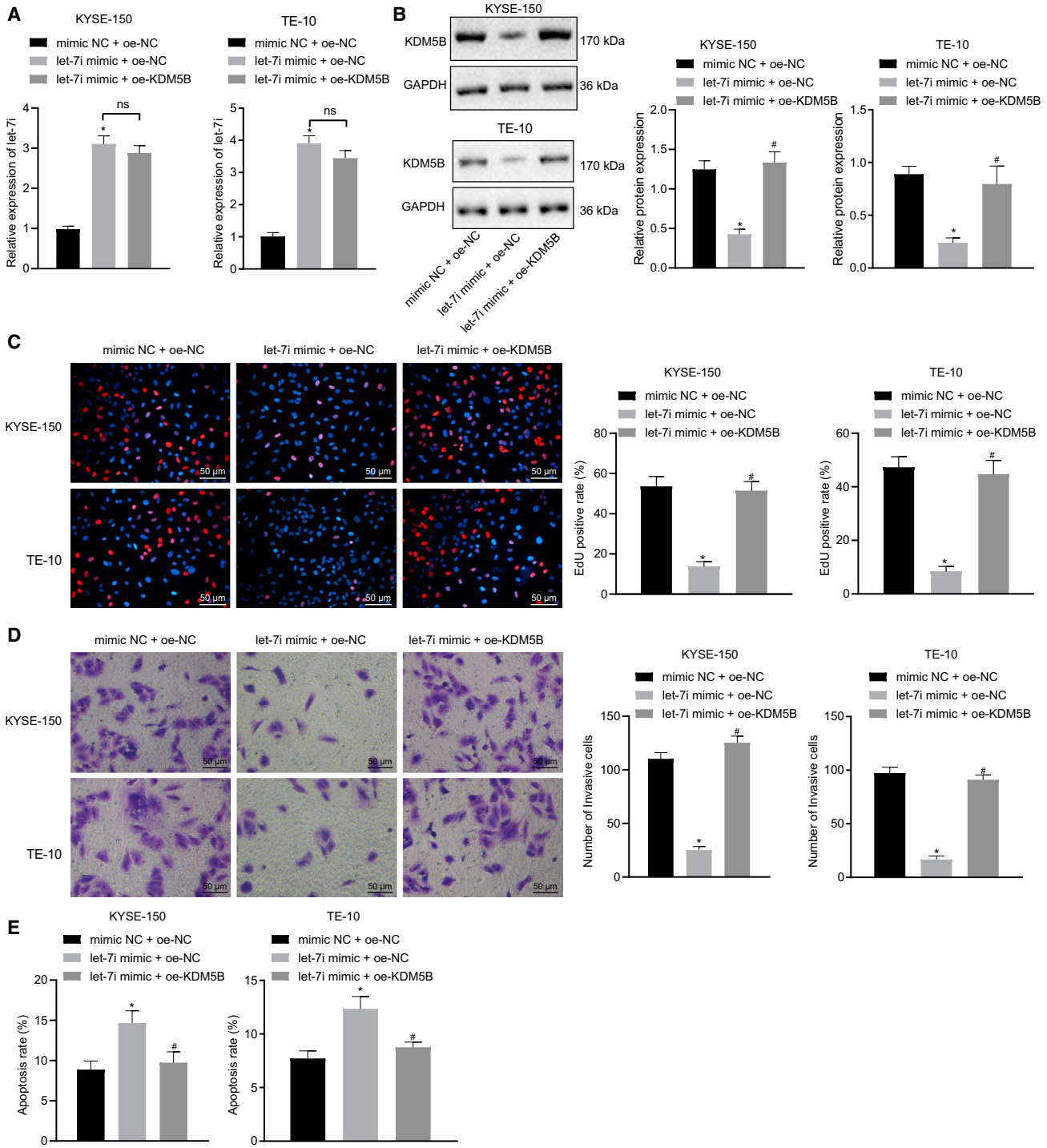

Figure 4. Overexpressing let-7i Suppresses Esophageal Cancer Progression via Targeting KDM5B *In Vitro*

In these experiments, the KYSE-150 and TE-10 cells were co-transfected with mimic NC and oe-NC, with let-7i mimic and oe-NC, or with let-7i mimic and oe-KDM5B. (A) Results of the qRT-PCR determining the expression of let-7i in KYSE-150 and TE-10 cells under the indicated conditions. (B) Representative images and results of the western blot analysis measuring the expression of KDM5B in KYSE-150 and TE-10 cells under the indicated conditions. (C) Representative images and analyzed results of the EdU proliferation assay evaluating the proliferation of KYSE-150 and TE-10 cells. (D) Representative images and analyzed result of the transwell invasion assay evaluating the invasion of KYSE-150 and TE-10 cells. (E) Results of the flow cytometry assessing the apoptosis in KYSE-150 and TE-10 cells under the indicated conditions. *$p < 0.05$ versus mimic NC + oe-NC group; #$p < 0.05$ versus let-7i mimic + oe-NC group; ns, no statistical significance.

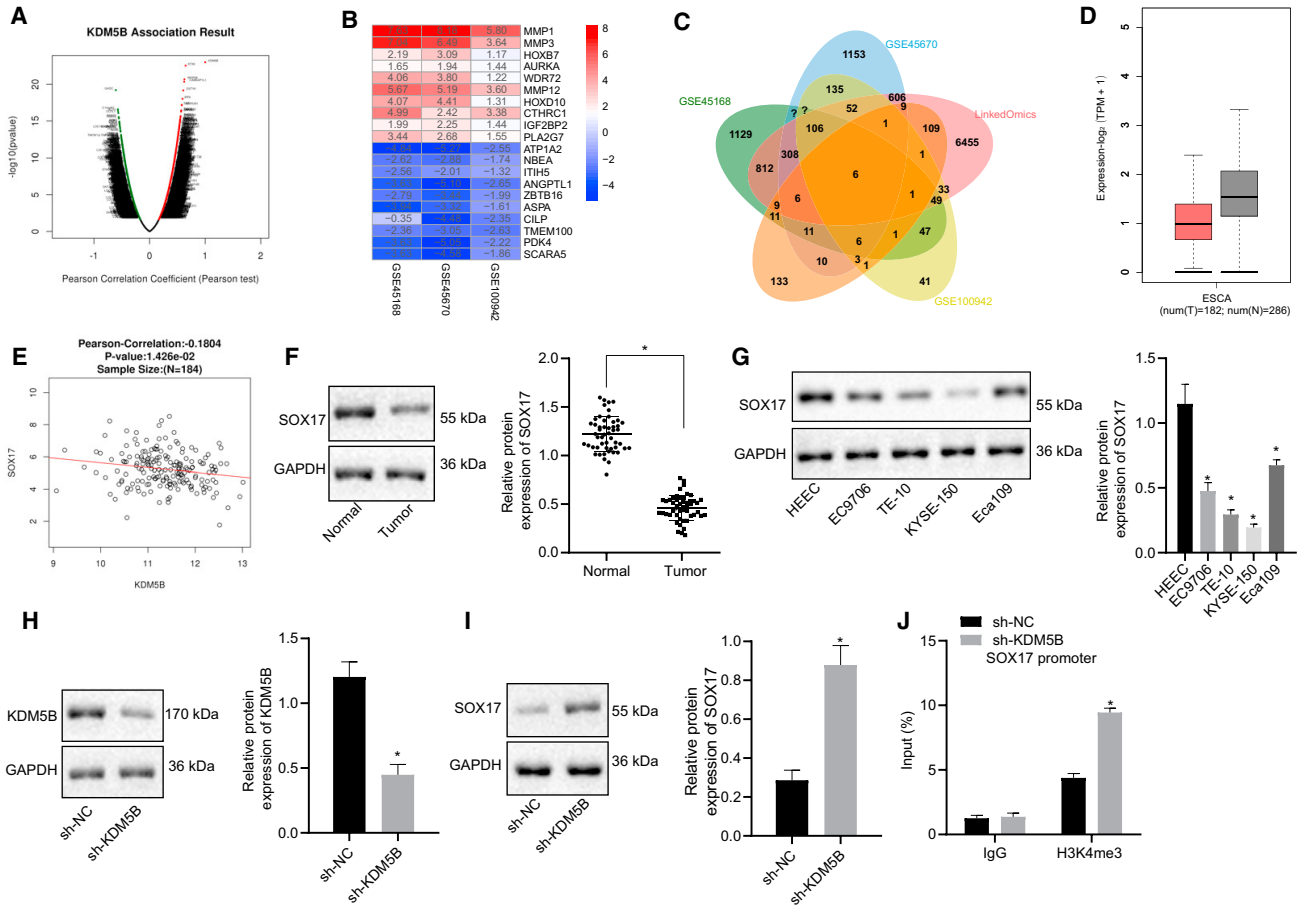

Figure 5. KDM5B Silencing Promotes H3K4me3 and Enhances the Expression of SOX17

(A) Heatmap obtained from LinkedOmics displaying KDM5B-related genes in esophageal cancer. Abscissa: correlation with KDM5B; ordinate: significance of correlation represented as −log(p). (B) Heatmap of top 10 upregulated and downregulated genes obtained from the datasets GSE45168, GSE45670, and GSE100942. (C) Venn diagram displaying the overlapped genes among KDM5B-related genes, DEGs from GEO datasets (GSE45168, GSE45670, and GSE100942), and human transcription factors; the intersection includes HOXB7, MEIS1, SOX17, TCF21, PBX1, and FOX. (D) Analyzed results from the GEPIA database presented as a box diagram displaying the downregulation of SOX17 in esophageal cancer. (E) Correlation between KDM5B and SOX17 in esophageal cancer analyzed by LinkedOmics ($r = -0.1804$, $p = 1.426E{-}02$). (F) Representative images and the results of the western blot analysis measuring the expression of SOX17 in esophageal tumors and adjacent normal tissues (n = 51). (G) Representative images and results of the western blot analysis measuring the expression of SOX17 in esophageal cancer cells and HEEC. (H) Representative images and results of the western blot analysis measuring the expression of KDM5B in the cells under the indicated conditions. (I) Representative images and results of the western blot analysis measuring the expression of SOX17 in the cells under the indicated conditions. (J) Results of the ChIP assay evaluating the level of H3K4me3 at the SOX17 promoter region in the cells under indicated conditions. *$p < 0.05$ versus normal, HEEC, or sh-NC group.

that KDM5B silencing repressed the cell invasion. However, KDM5B deficiency did not impair cell invasion in SOX17-depleted cells (Figure 6C). Furthermore, we also evaluated cell apoptosis by flow cytometry, finding that ablation of KDM5B resulted in increased apoptosis, whereas that increase could be counteracted by silencing of SOX17 (Figure 6D). These observations suggested that KDM5B could promote esophageal cancer progression by suppressing expression of SOX17.

SOX17 Overexpression Suppresses Esophageal Cancer Proliferation and Invasion via Inhibiting GREB1

We then attempted to clarify how SOX17 was involved in the progression of esophageal cancer. Interestingly, recent evidence has demonstrated that the expression of GREB1 was regulated by SOX17,[24] and results obtained from the GEPIA database also suggested an upregulated expression of GREB1 in esophageal cancer (Figure 7A). Importantly, accumulating evidence has suggested that GREB1 exhibits a promotive effect on tumor progression.[25,26] Thus, we speculated that GREB1 might be involved in SOX17-mediated tumor suppression. To test that, we determined the expression of GREB1 in esophageal tumors and esophageal cancer cells by western blot analysis. The results showed that, compared with adjacent healthy tissue or HEEC, GREB1 was upregulated in esophageal tumor tissues and esophageal cancer cells (Figures 7B and 7C). Moreover, we detected expression of GREB1 in cells transfected with SOX17-overexpression plasmid

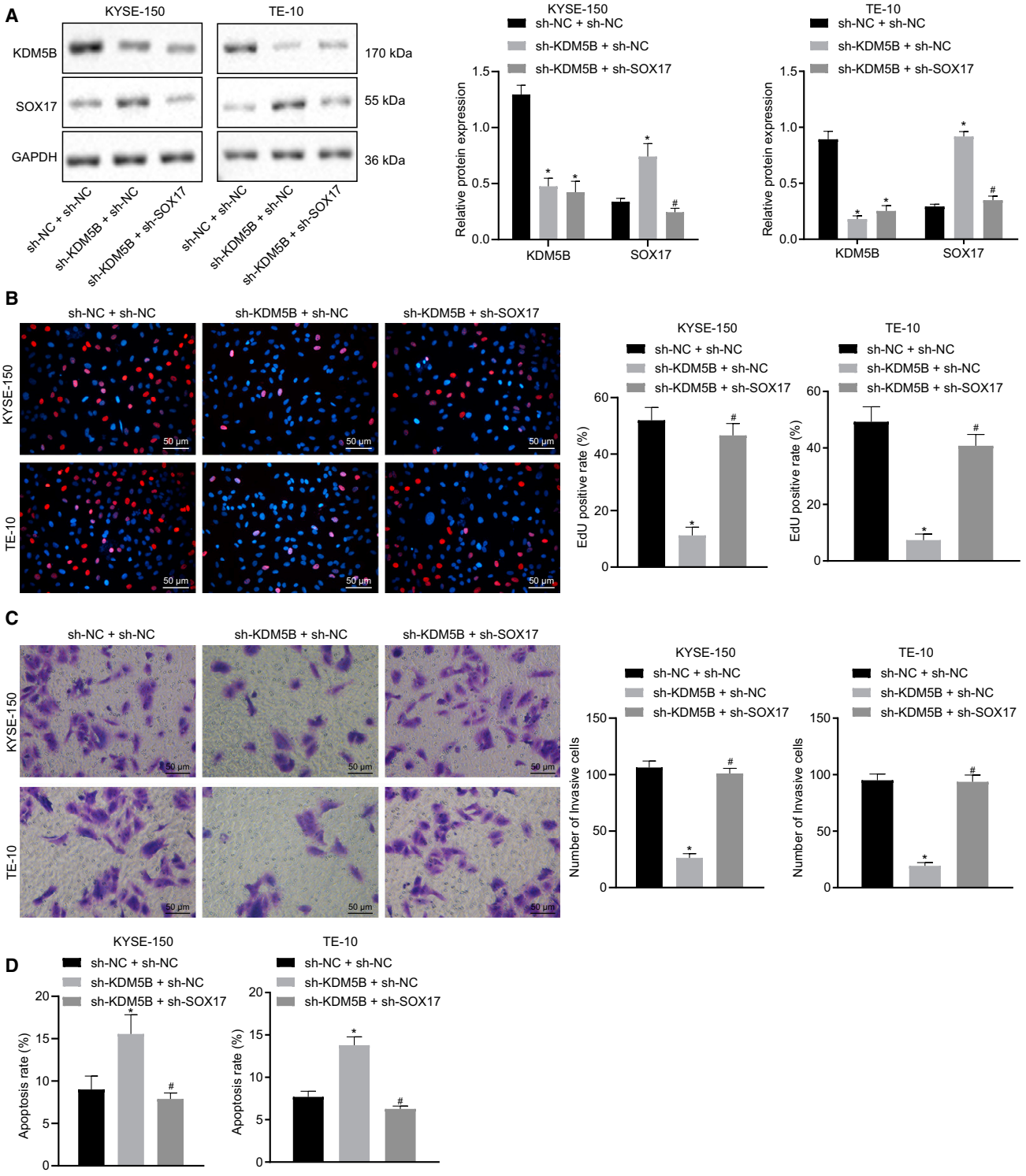

Figure 6. KDM5B Knockdown Suppresses Esophageal Cancer Cell Proliferation and Invasion via Enhancing SOX17

In these experiments, the KYSE-150 and TE-10 cells were co-transfected with sh-NC and sh-NC, with sh-KDM5B and sh-NC, or with sh-KDM5B and sh-SOX17. (A) Representative images and data from the western blot analysis measuring the expression of KDM5B and SOX17 in KYSE-150 and TE-10 cells. (B) Representative images

(legend continued on next page)

(oe-SOX17), finding that GREB1 was significantly downregulated in cells overexpressing SOX17 (Figures 7D and 7E). To further understand the role of SOX17-regulated GREB1 in the pathogenesis of esophageal cancer, SOX17 and/or GREB1 was overexpressed in esophageal cancer cells. After validating the efficiency by western blot analysis (Figure 7F), we examined the cell proliferation with an EdU assay. The results showed that SOX17 overexpression resulted in decreased cell proliferation and that this reduced proliferation rate was rescued by GREB1 overexpression (Figure 7G). These findings suggest that SOX17 inhibits esophageal cancer cell growth by suppressing GREB1. We then performed the transwell assay to investigate how SOX17 and GREB1 were involved in esophageal cancer cell invasion, finding reduced invasive potency in SOX17-overexpressing cells, which was rescued by GREB1 overexpression (Figure 7H). These results indicate that SOX17 suppresses esophageal cancer cell invasion by inhibiting GREB1 expression. The results of the flow cytometry exhibited increased cell apoptosis in response to SOX17 overexpression. However, overexpressing GREB1 could diminish the cell apoptosis enhanced by SOX17 overexpression (Figure 7I). These results indicate that SOX17 promotes esophageal cancer cell apoptosis by regulating GREB1. Taken together, our findings suggest that SOX17 impairs esophageal cancer progression *in vitro* by suppressing GREB1.

let-7i Downregulates GREB1 to Inhibit the Progression of Esophageal Cancer in a KDM5B/SOX17-Dependent Manner

To investigate whether let-7i suppresses the progression of esophageal cancer by regulating GREB1, we overexpressed let-7i and/or GREB1 in esophageal cancer cells. The results of the qRT-PCR demonstrated that let-7i was upregulated in cells transfected with let-7i mimic, whereas GREB1 overexpression did not affect the expression of let-7i (Figure 8A). We then determined the expression of KDM5B, SOX17, and GREB1 in those cells by western blot analysis, finding that the cells transfected with let-7i mimic expressed lower levels of KDM5B and GREB1 but more SOX17, whereas GREB1 overexpression did not affect the expression levels of KDM5B and SOX17 (Figure 8B). These findings indicated that GREB1 was the downstream gene of the let-7i/KDM5B/SOX17 axis and was modulated by the let-7i-regulated KDM5B/SOX17 axis. We next evaluated proliferation in those cells via the EdU assay. We observed that let-7i overexpression resulted in a reduced cell proliferation rate, whereas GREB1 overexpression compromised the suppressive effect of let-7i overexpression on cell proliferation (Figure 8C). Moreover, the result of the transwell invasion assay displayed that let-7i overexpression impaired the invasion of esophageal cancer cells, and that this impaired cell invasion was rescued by GREB1 overexpression (Figure 8D). Furthermore, cell apoptosis was evaluated in those cells via flow cytometry, which showed that let-7i overexpression resulted in increased cellular apoptosis. However, overexpressing GREB1 contributed to reversing the pro-apoptotic effect of let-7i on esophageal cancer cells (Figure 8E). Together, these findings suggest that let-7i suppressed esophageal cancer progression *in vitro* by downregulating GREB1 in a KDM5B/SOX17-dependent manner.

let-7i Suppresses Esophageal Tumorigenesis *In Vivo* by Regulating the KDM5B/SOX17/GREB1 Axis

Because our data demonstrated that let-7i exerts inhibitory effects on esophageal cancer cell growth and proliferation *in vitro*, we further validated those findings *in vivo* using a tumor xenograft model in a nude mice. For that purpose, we overexpressed let-7i and/or GREB1 using let-7i agomir and oe-GREB1 in esophageal cancer cells and then injected those cells into the nude mice. The results of qRT-PCR in tumor tissues showed that let-7i agomir significantly increased the expression of let-7i, whereas GREB1 overexpression did not affect let-7i expression (Figure 9A). We then detected the expression of KDM5B, SOX17, and GREB1 in those tumors, finding that let-7i overexpression reduced the expression of KDM5B and GREB1 but increased the expression of SOX17. In addition, GREB1 overexpression did not affect expression of KDM5B and SOX17 (Figure 9B). We further compared the xenograft tumors from each group. The results showed that let-7i overexpression impaired tumorigenesis, as reflected by smaller tumor size and lower tumor weight (Figure 9C). However, tumor size and tumor weight were increased in response to GREB1 overexpression in the presence of let-7i (Figure 9D). These findings demonstrated that let-7i inhibited esophageal tumorigenesis by inhibiting GREB1 in a KDM5B/SOX17-dependent manner.

DISCUSSION

Esophageal cancer is the sixth most-lethal human digestive tract malignancy.[1] Despite advanced achievements in its diagnosis and treatment, the 5-year survival rate for patients with esophageal cancer, especially for those who were diagnosed at advanced stage, still needs improvement.[1] Thus, novel and effective therapeutic strategies are urgently needed, which require a better understanding of the pathogenesis of this malignancy.

Initially, we identified the downregulation of let-7i in esophageal tumor tissues and showed that downregulation was correlated with an advanced TNM stage, the presence of LNM, and poor prognosis. This finding was supported by a previous study. which had shown reduced let-7i in esophageal carcinoma.[21] Moreover, we have shown that overexpressing let-7i suppressed esophageal cancer cell proliferation and invasion and promoted its apoptosis. In alignment with our findings, others have demonstrated that downregulated let-7i suppresses esophageal cancer cell proliferation and promotes cell apoptosis.[21] In addition, the anti-tumor role of let-7i has been demonstrated in other gastrointestinal tumors, such as gastric cancer and colon

and results of the EdU assay evaluating the proliferation of KYSE-150 and TY-10 cells under the indicated conditions. (C) Representative images and data from the transwell assay evaluating the invasion potency of KYSE-150 and TY-10 cells under the indicated conditions. (D) Results of the flow cytometry assessing the apoptosis of KYSE-150 and TY-10 cells under the indicated conditions. *$p < 0.05$ versus sh-NC + sh-NC group; #$p < 0.05$ versus sh-KDM5B + sh-NC group.

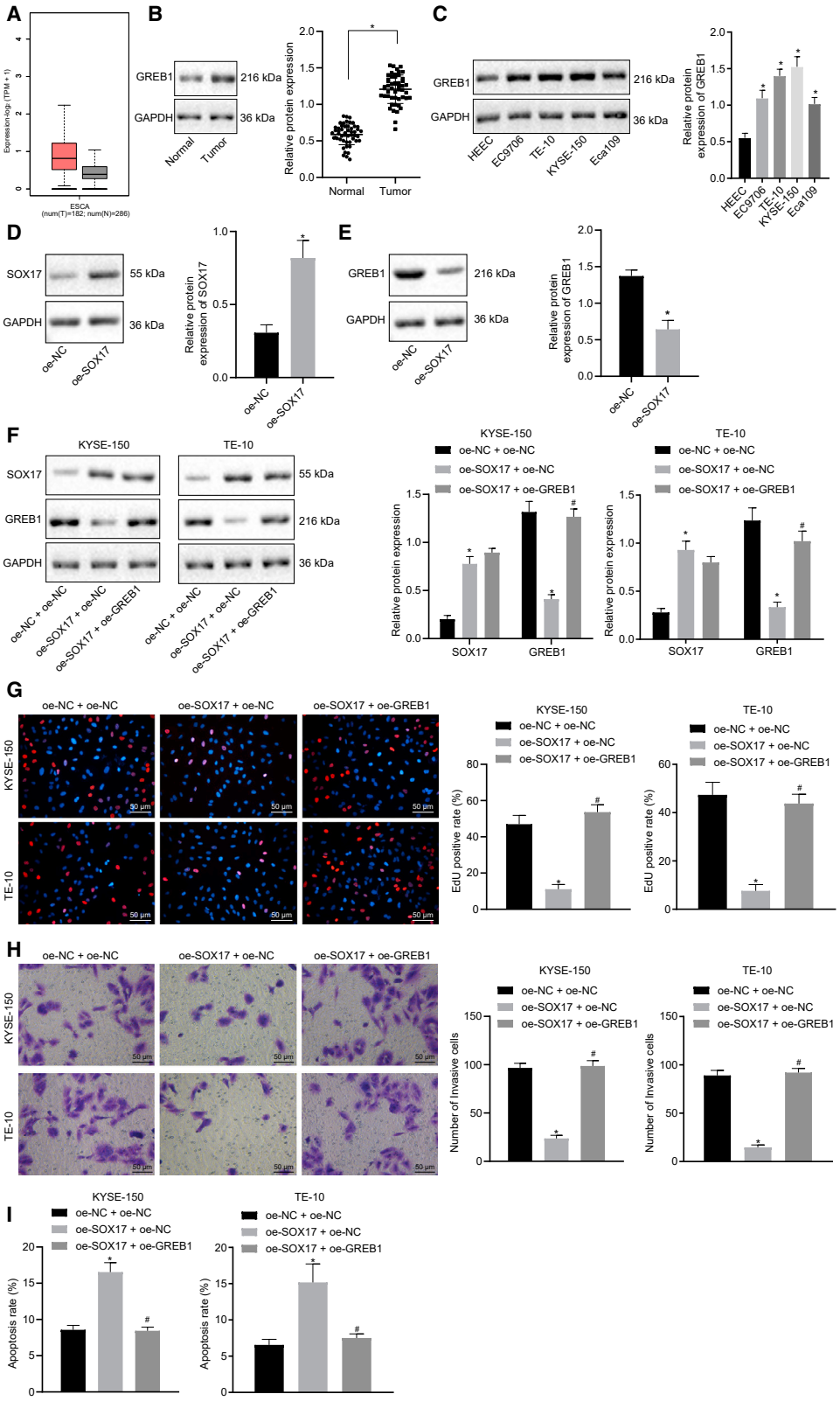

(legend on next page)

cancer.[27,28] Moreover, a recent study revealed that let-7i exerts inhibitory effects on the mobility and growth of bladder cancer cells.[11]

Our research validated that let-7i could target KDM5B, raising the possibility that upregulation of KDM5B in esophageal cancer tissues is a consequence of the downregulation of let-7i. Accumulating evidence has demonstrated that KDM5B epigenetically suppresses the expression of tumor-suppressor genes by regulating the H3K4me3 level.[29] For instance, in lung cancer, upregulated KDM5B resulted in decreased expression of p53,[30] which is a well-established tumor-suppressor gene.[31] Moreover, KDM5B overexpression has also been related to increased cancer cell proliferation and invasion in liver and gastric cancers.[32–34] Cui et al.[13] demonstrated that KDM5B was upregulated in esophageal squamous cell carcinoma cells and could promote the development of esophageal squamous cell carcinoma, which is consistent with our present results. Moreover, our *in vitro* study indicated that KDM5B overexpression compromised the inhibitory effects of let-7i in esophageal cancer progression, suggesting that let-7i suppressed esophageal cancer progression by targeting KDM5B. This is similar to the mechanism reported by Shi et al.,[27] in which enforced expression of let-7i resulted in inhibited cell migration and invasion in gastric cancer by directly targeting COL1A1.

Through bioinformatic analysis, we found that SOX17, a tumor suppressor of esophageal cancer,[23] was downregulated in esophageal tumor tissues. Others have provided evidence that SOX17 exerts a suppressive role in gastrointestinal tumorigenesis.[35,36] In addition, a previous study[22] has shown that SOX17 could be regulated by KDM5B. Our new data suggest that SOX17 could be epigenetically suppressed by KDM5B because we found that KDM5B deficiency could enhance the recruitment of H3K4me3 in the SOX17 promoter region and hence elevated SOX17 expression. Furthermore, our experiments demonstrated that silencing KDM5B could inhibit cancer cell growth, invasion, and survival by upregulating SOX17. This was consistently supported by previous findings that upregulation of SOX17 repressed cancer cell proliferation, invasion, and migration in breast cancer.[37]

It has been demonstrated elsewhere that expression of the tumor-promoter GREB1[26] could be regulated by SOX17.[24] In addition, accumulating evidence has revealed that GREB1 promotes cancer cell proliferation, invasion, and survival in multiple types of cancers.[26,38] Recent evidence has also consistently revealed that upregulated GREB1 accelerates tumor progression in ovarian cancer.[39] The present study provides evidence that SOX17 negatively regulates GREB1 expression and that the inhibitory effect of SOX17 on esophageal cancer progression is GREB1 dependent. Furthermore, we also observed that the inhibitory effect of let-7i on esophageal cancer progression could be compromised by overexpressing GREB1 in esophageal cancer cells, a result that was further validated *in vivo*. Taken together, our results suggest that let-7i suppresses esophageal cancer progression by targeting KDM5B and inducing SOX17-dependent downregulation of SOX17.

In conclusion, our study demonstrates that let-7i exerts an antitumor effect on esophageal cancer cells, which were mechanistically associated with the KDM5B/SOX17/GREB1 axis. These findings should contribute to the development of novel therapeutic targets based on that axis. However, we concede that few patient samples were studied and that a larger sample size would reduce sampling errors. In addition, it remains possible that other pathways are involved in the let-7i-mediated progression of esophageal cancer, which warrants further investigations.

MATERIALS AND METHODS

Ethical Statement

This study was performed under the approval of the Ethics Committee of The First Affiliated Hospital of Zhengzhou University, and all participating patients signed informed consent documents. All animal studies were accomplished under the protocol approved by the Institutional Animal Care and Use Committee of The First Affiliated Hospital of Zhengzhou University.

Patient and Specimen Collection

Fifty-one cases of esophageal cancer tissues and adjacent healthy tissues were collected from patients who underwent surgery at The First Affiliated Hospital of Zhengzhou University between January 2017 and January 2019 (n = 51; males, 30; females, 21). The age of the participants ranged from 39 years to 70 years, with a median of 58.86 ± 10.42 years. Patients meeting the following criteria were recruited: (1) patients received surgery; (2) patients did not receive radiotherapy, chemotherapy, or immunotherapy before surgery; and (3) the clinical information of the participants was complete. Patients whose specimen was not evaluated by a pathologist or patients who had received radiotherapy or chemotherapy were excluded from this study.

Immunohistochemistry Analysis

Tumor tissues were fixed with paraformaldehyde and embedded in paraffin. Then the paraffin-embedded sections were stained with

Figure 7. SOX17 Overexpression Suppresses Esophageal Cancer Cell Proliferation and Invasion via Inhibiting GREB1

(A) Analyzed results obtained from the GEPIA database presented as a box diagram displaying the upregulation of GREB1 in esophageal cancer. (B) Representative images and results of the western blot analysis measuring the expression of GREB1 in esophageal tumors and adjacent normal tissues. (C) Representative images and results of the western blot analysis evaluating the expression of GREB1 in esophageal cancer cells and normal esophageal epithelial cells. (D and E) Representative images and results of the western blot analysis measuring the expression of SOX17 (D) and GREB1 (E) in esophageal cancer cells under the indicated conditions. (F) Representative images and results of the western blot analysis examining the expression of SOX17 and GREB1 in KYSE-150 and TY-10 cells under the indicated conditions. (G) Results of the EdU assay evaluating the proliferation of KYSE-150 and TY-10 cells under the indicated conditions. (H) Representative images and results of the transwell assay evaluating the invasion of KYSE-150 and TY-10 cells under the indicated conditions. (I) Results of the flow cytometry assessing the apoptosis of KYSE-150 and TY-10 cells under the indicated conditions. *$p < 0.05$ versus oe-NC + oe-NC group; #$p < 0.05$ versus oe-SOX17 + oe-NC.

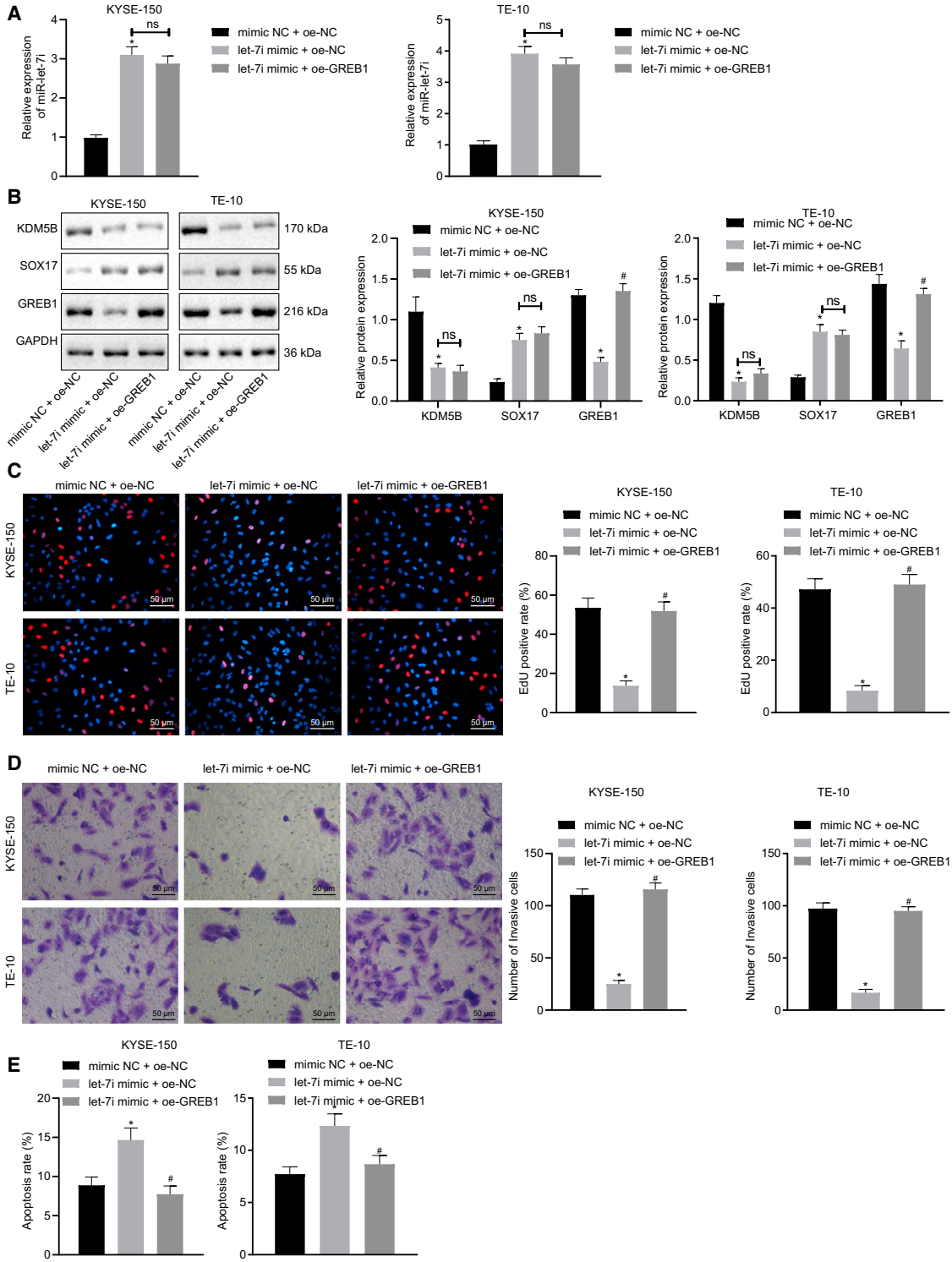

Figure 8. let-7i Downregulates GREB1 to Repress the Progression of Esophageal Cancer *In Vitro* in a KDM5B/SOX17-Dependent Manner

In these experiments, the KYSE-150 and TE-10 cells were co-transfected with mimic NC and oe-NC, with let-7i mimic and oe-NC, or with the let-7i mimic and oe-GREB1. (A) Results of the qRT-PCR determining the expression of let-7i in KYSE-150 and TY-10 cells under the indicated conditions. (B) Representative images and results of the western blot analysis measuring the expression of KBM5B, SOX17, and GREB1 in KYSE-150 and TY-10 cells under the indicated conditions. (C) Representative images and

(legend continued on next page)

the KDM5B antibody (1:250; ab244220, Abcam, Cambridge, MA, USA), as previously described.[40] After incubation with a horseradish peroxidase (HRP)-conjugated secondary antibody (0343-10000U, ImunBio Biotechnology, Beijing, China), the sections were visualized with 3,3′-diaminobenzidine (DAB) reagent (ST033, Guangzhou Whiga Biotechnology, Guangzhou, China), and the nuclei were counterstained with hematoxylin (PT001; Bogoo Biological Technology, Shanghai, China). The sections were then dehydrated, mounted, and observed under a microscope.

Cell Culture and Treatment

HEEC and 4 esophageal cancer cell lines—EC9706, Eca109, KYSE-150, and TE-102—were purchased from ATCC (Manassas, VA, USA). After thawing, the cells were cultured with Dulbecco's modified Eagle's medium containing 10% fetal bovine serum (26140079; Gibco, Carlsbad, CA, USA) and 1% penicillin-streptomycin at 37°C with 5% CO_2. The medium was replaced every day. When cell confluence reached 60%–70%, cell transfection was performed based on the instructions of the Lipofectamine 2000 kit (Thermo Fisher Scientific, Waltham, MA, USA). The plasmids, including sh-NC, sh-KDM5B, sh-SOX17, oe-NC, oe-KDM5B, oe-SOX17, and oe-GREB1, as well as the mimic NC, let-7i mimic, inhibitor-NC, and let-7i inhibitor were all purchased from Sino Biological (Beijing, China). After 48 h of transfection, the cells were employed for subsequent experiments.

qRT-PCR

Total RNA was extracted using commercially available reagents. For quantification of let-7i, miRNA First Strand cDNA Synthesis (Tailing Reaction) kit (B532451; Sangon Biotech, Shanghai, China) was adopted to generate cDNA. The cDNA was amplified on an ABI 7500 RT-PCR system (Thermo Fisher Scientific) using Fast SYBRT Green PCR kit (Thermo Fisher Scientific). U6 was used as internal control, and the relative gene expression was calculated using the $2^{-\Delta\Delta Ct}$ method. Primers used in this study are listed in Table 2.

EdU Proliferation Assay

The EdU proliferation assay was conducted as previously reported.[41] In brief, cells were seeded into 24-well plates with triplicates in each group and cultured for the indicated periods. On the day of experiment, the cells were treated with 10 μM EdU reagent for 2 h at 37°C, followed by fixation with 4% paraformaldehyde for 15 min at room temperature. After that, the cells were washed twice with phosphate-buffered saline (PBS) containing 3% bovine serum albumin (BSA) and permeabilized with 0.5% Triton X-100 for 20 min at room temperature. At the completion of permeabilization, the cells were washed twice with PBS containing 3% BSA. Then, 100 μL of staining solution was added into each well, and the cells were incubated for 30 min in the dark at room temperature. Cells were stained with 4′,6-diamidino-2-phenylindole (DAPI) for 5 min. When the staining was completed, the cells were observed under a FM-600 immunofluorescence microscope (PUDA), and images were taken. The numbers of EdU-positive and EdU-negative (DAPI-positive) cells were counted in random fields, which were calculated as the percentage of EdU-positive cells using the formula: EdU-positive rate (5) = EdU-positive cell count/(EdU-positive cell count + EdU-negative cell count) × 100%.

Western Blot Analysis

Cells were solubilized in radioimmunoprecipitation assay lysis buffer supplemented with protease inhibitors (Boster) and cleared cell lysate was collected by centrifugation at 4°C. Protein concentration was determined using the bicinchoninic acid protein assay kit (Boster Biological Technology, Wuhan, China). Protein electrophoresis was performed using SDS-PAGE gels (10%), and the separated proteins were transferred onto polyvinylidene fluoride membranes. The membranes were blocked with 5% BSA for 2 h at room temperature and then incubated with primary antibodies at 4°C overnight: anti-KDM5B (ab181089, Abcam, 1:2,000), SOX17 (ab224637, 1:500), and GREB1 (ab72999, 1:1,000). The next day, the membranes were washed with Tris-buffered saline with Tween (3 times, 10 min each) and incubated with HRP-conjugated secondary antibody (goat anti-Rabbit immunoglobulin G [IgG], ab205719, Abcam, 1:2,000) for 1 h at room temperature. The membranes were then developed with ECL reagent (MilliporeSigma, Burlington, MA, USA). The results were quantified using ImageJ (NIH, Bethesda, MD, USA), and the intensity values were normalized to β-actin.

Transwell Invasion Assay

A transwell invasion assay was conducted to evaluate cell mobility as previously reported.[42] In brief, cells starved for 12 h were suspended in serum-free medium, and 100 μL of harvested cell suspension (1×10^5 cells/mL) was seeded into the upper chamber of the transwell inserts coated with Matrigel. A medium containing 10% FBS was added to the lower chamber. After 24 h of incubation at 37°C, Matrigel and uninvaded cells were removed by cotton swab, and the invaded cells were fixed with 1% toluidine blue O solution. The cells were then monitored under an inverted microscope (Carl Zeiss, Oberkochen, Germany), and invaded cells were counted and recorded from 5 randomly selected fields of each insert.

Annexin V Apoptosis Assay

Cell apoptosis was evaluated by flow-cytometry-based assay, as previously reported.[43] In general, cells were collected by centrifugation (2,000 × *g*, 5 min), washed with ice-cold PBS twice, and suspended in 400 μL of 1 × binding buffer. After that, 5 μL of Annexin V-fluorescein isothiocyanate (FITC) was added into the cell suspension and incubated for 15 min at 4°C. The cells were then stained with the addition of 5 μL propidium iodide (PI) for 5 min at 4°C. Cellular

results of the EdU assay evaluating cell proliferation in KYSE-150 and TY-10 cells under the indicated conditions. (D) Representative images and results of the transwell assay evaluating the invasive potency of KYSE-150 and TY-10 cells under the indicated conditions. (E) Results of flow cytometry examining the cellular apoptosis in KYSE-150 and TY-10 cells under the indicated conditions. *$p < 0.05$ versus mimic NC + oe-NC group, $p < 0.05$; #$p < 0.05$ versus let-7i mimic + oe-NC group; ns, no statistical significance.

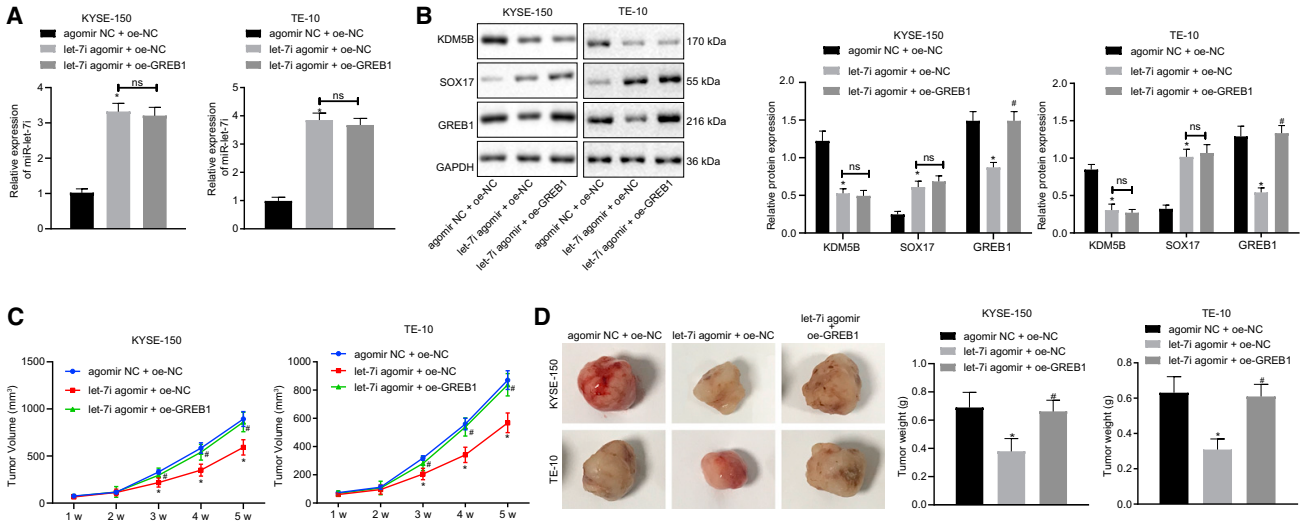

Figure 9. let-7i Suppresses Esophageal Tumorigenesis *In Vivo* by Regulating the KDM5B/SOX17/GREB1 Axis

In these experiments, the KYSE-150 and TE-10 cells stably co-transduced with agomir NC and oe-NC, with let-7i agomir and oe-NC, or with both let-7i agomir and oe-GREB1 were delivered into nude mice. (A) Results of the qRT-PCR determining the expression of let-7i in xenografts from each group. (B) Representative images and results of the western blot analysis measuring the expression of KDM5B, SOX17, and GREB1 in xenografts from each group. (C) Tumor growth curve represented by tumor volume at the indicated time point. (D) Representative images of xenograft tumors and analyzed tumor weights from each group. *p < 0.05 versus agomir NC + oe-NC group; #p < 0.05 versus let-7i + oe-NC group; ns, no statistical significance.

apoptosis was then determined by a flow cytometer (Calibur, fluorescence-activated cell sorting [FACS]; BD Biosciences, San Jose, CA, USA).

Dual-Luciferase Reporter Gene Assay

Cells from each group were seeded into 6-well plates at a concentration of 2×10^5 cells/well and subjected to transfection. After 48 h of transfection, cells were collected, and luciferase activities were detected using dual luciferase assay kit (D0010, Solarbio, Beijing, China) according to the manufacturer's instruction. The luciferase activated reflected by luminescence was determined with Glomax20/20 luminometer (E5311, Promega, Madison, WI, USA).

ChIP Assay

The ChIP assay was performed with a ChIP kit (MilliporeSigma) according to the manufacturer's instruction. In brief, cells were treated with 1% formaldehyde for 10 min at room temperature to crosslink DNA and proteins. The DNA was then subjected to sonication (120 W, 15 cycles of 2 s on and 5 s off) to generate DNA fragments. The cell debris was then removed by centrifugation (13,000 × *g* at 4°C). The DNA-protein complexes in the supernatant were divided into 3 portions and incubated overnight at 4°C with rabbit anti-RNA polymerase II IgG, rabbit IgG, and rabbit anti-H3K4me3 IgG (ab185637, Abcam, 1:100), respectively. The next day, antibody-enriched DNA-protein complexes were precipitated by protein agarose and collected by brief centrifugation. The complexes were then subjected to washing and decrosslinking (65°C overnight), and the DNA fragments were then purified and amplified for SOX17 promoter detection via qRT-PCR.

Tumor Xenograft in Nude Mice

Female nude mice (5–6 weeks old) purchased from Shanghai SLAC laboratory (SLAC, Shanghai, China) were used to establish a tumor xenograft mouse model. Cells under indicated conditions (80%–90% confluence) were suspended in PBS and injected subcutaneously into the armpit of nude mice at a dose of 2×10^5 cells/mouse (n = 8). The tumor volume was measured weekly according to the formula: $(a \times b^2)/2$, where a and b represent the tumor length and width (in millimeters), respectively. To avoid severe discomfort of the mice in each group, animals were sacrificed after 5 weeks. Tumor volume in nude mice was plotted against time.

Statistical Analysis

All results were analyzed with SPSS software (21.0 version, IBM, Armonk, NY, USA) and were presented as mean values ± standard deviation of at least 3 independent experiments. Data between 2 groups were compared using paired t test (cancer tissues and adjacent healthy tissues) or unpaired t test (other data). Comparisons among multiple groups were performed by one-way analysis of variance (ANOVA) with Tukey's post hoc test. Comparisons over time were conducted with repeated-measurement ANOVA, followed by Bonferroni post hoc test. With the median of the let-7i expression in the tissues of patients with esophageal cancer as the cutoff point, those patients were assigned into subgroups of patients with low and high let-7i expressions. The overall survival time for patients with esophageal cancer was analyzed by Kaplan-Meier analysis, and the survival difference between the 2 groups was analyzed by log-rank. A value of $p < 0.05$ was considered as statistically significant.

Table 2. Primer Sequence for qRT-PCR

Gene	Sequence	
let-7i	Forward	5′-CCTAGAAGGAATTGAGGGGAGT-3′
	Reverse	5′-TGGCATTTAACTGCTGAAAGAA-3′
U6	Forward	5′-ACAGAGAAGATTAGCATGGCC-3′
	Reverse	5′-GACCAATTCTCGATTTGTGCG-3′

Note: qRT-PCR, quantitative reverse transcriptase polymerase chain reaction.

AUTHOR CONTRIBUTIONS

Y.Y. conceived, and together with W.L. and B.W., designed and conducted the experiments. K.W., D.L., and D.Z. were involved in data collection. C.Z. and F.W. performed the statistical analysis and preparation of figures. Y.F. drafted the paper. S.Z., Y.Y., W.L., and B.W. contributed substantially to its revision. All authors read and approved the final manuscript.

CONFLICTS OF INTEREST

The authors declare no competing interests.

ACKNOWLEDGMENTS

We acknowledge and appreciate our colleagues for their valuable efforts and comments on this paper. This work was supported by the Youth Foundation of the National Natural Science Foundation of China (No. 81702971), the Key Scientific Research Projects of Colleges and Universities of Henan Province (No. 18A320054), the Science and Technology Research Projects of Henan Province (No. 182102310116), and the Youth Talent Lifting Projects of Henan Province (No. 2020HYTP050).

REFERENCES

1. Testa, U., Castelli, G., and Pelosi, E. (2017). Esophageal cancer: genomic and molecular characterization, stem cell compartment and clonal evolution. Medicines (Basel) *4*, 67.
2. Allegra, A., Musolino, C., Tonacci, A., Pioggia, G., and Gangemi, S. (2020). Interactions between the MicroRNAs and microbiota in cancer development: roles and therapeutic opportunities. Cancers (Basel) *12*, 805.
3. Roscigno, G., Cirella, A., Affinito, A., Quintavalle, C., Scognamiglio, I., Palma, F., Ingenito, F., Nuzzo, S., De Micco, F., Cuccuru, A., et al. (2020). miR-216a acts as a negative regulator of breast cancer by modulating stemness properties and tumor microenvironment. Int. J. Mol. Sci. *21*, 2313.
4. Acunzo, M., Romano, G., Wernicke, D., and Croce, C.M. (2015). MicroRNA and cancer-—a brief overview. Adv. Biol. Regul. *57*, 1–9.
5. Lu, H.B. (2018). MicroRNA-556-3p promotes the progression of esophageal cancer via targeting DAB2IP. Eur. Rev. Med. Pharmacol. Sci. *22*, 6816–6823.
6. Hsu, W.C., Li, W.M., Lee, Y.C., Huang, A.M., Chang, L.L., Lin, H.H., Wu, W.J., Li, C.C., Liang, P.I., and Ke, H.L. (2020). MicroRNA-145 suppresses cell migration and invasion in upper tract urothelial carcinoma by targeting ARF6. FASEB J. *34*, 5975–5992.
7. Williams, M., Cheng, Y.Y., Blenkiron, C., and Reid, G. (2017). Exploring Mechanisms of MicroRNA Downregulation in Cancer. MicroRNA *6*, 2–16.
8. Liu, Q., Lv, G.D., Qin, X., Gen, Y.H., Zheng, S.T., Liu, T., and Lu, X.M. (2012). Role of microRNA let-7 and effect to HMGA2 in esophageal squamous cell carcinoma. Mol. Biol. Rep. *39*, 1239–1246.
9. Li, X.X., Di, X., Cong, S., Wang, Y., and Wang, K. (2018). The role of let-7 and HMGA2 in the occurrence and development of lung cancer: a systematic review and meta-analysis. Eur. Rev. Med. Pharmacol. Sci. *22*, 8353–8366.
10. Peng, F., Li, T.T., Wang, K.L., Xiao, G.Q., Wang, J.H., Zhao, H.D., Kang, Z.J., Fan, W.J., Zhu, L.L., Li, M., et al. (2017). H19/let-7/LIN28 reciprocal negative regulatory circuit promotes breast cancer stem cell maintenance. Cell Death Dis. *8*, e2569.
11. Qin, M.M., Chai, X., Huang, H.B., Feng, G., Li, X.N., Zhang, J., Zheng, R., Liu, X.C., and Pu, C. (2019). let-7i inhibits proliferation and migration of bladder cancer cells by targeting HMGA1. BMC Urol. *19*, 53.
12. Sun, J., Pan, L.M., Chen, L.B., and Wang, Y. (2017). LncRNA XIST promotes human lung adenocarcinoma cells to cisplatin resistance via let-7i/BAG-1 axis. Cell Cycle *16*, 2100–2107.
13. Cui, G., Liu, D., Li, W., Li, Y., Liang, Y., Shi, W., and Zhao, S. (2017). Original Research: miR-194 inhibits proliferation and invasion and promotes apoptosis by targeting KDM5B in esophageal squamous cell carcinoma cells. Exp. Biol. Med. (Maywood) *242*, 45–52.
14. Xhabija, B., and Kidder, B.L. (2019). KDM5B is a master regulator of the H3K4-methylome in stem cells, development and cancer. Semin. Cancer Biol. *57*, 79–85.
15. Yamane, K., Tateishi, K., Klose, R.J., Fang, J., Fabrizio, L.A., Erdjument-Bromage, H., Taylor-Papadimitriou, J., Tempst, P., and Zhang, Y. (2007). PLU-1 is an H3K4 demethylase involved in transcriptional repression and breast cancer cell proliferation. Mol. Cell *25*, 801–812.
16. Hayami, S., Yoshimatsu, M., Veerakumarasivam, A., Unoki, M., Iwai, Y., Tsunoda, T., Field, H.I., Kelly, J.D., Neal, D.E., Yamaue, H., et al. (2010). Overexpression of the JmjC histone demethylase KDM5B in human carcinogenesis: involvement in the proliferation of cancer cells through the E2F/RB pathway. Mol. Cancer *9*, 59.
17. Reimer, D., Sadr, S., Wiedemair, A., Stadlmann, S., Concin, N., Hofstetter, G., Müller-Holzner, E., Marth, C., and Zeimet, A.G. (2007). Clinical relevance of E2F family members in ovarian cancer–an evaluation in a training set of 77 patients. Clin. Cancer Res. *13*, 144–151.
18. Mitra, D., Das, P.M., Huynh, F.C., and Jones, F.E. (2011). Jumonji/ARID1 B (JARID1B) protein promotes breast tumor cell cycle progression through epigenetic repression of microRNA let-7e. J. Biol. Chem. *286*, 40531–40535.
19. Wang, W., Corrigan-Cummins, M., Barber, E.A., Saleh, L.M., Zingone, A., Ghafoor, A., Costello, R., Zhang, Y., Kurlander, R.J., Korde, N., et al. (2015). Aberrant levels of miRNAs in bone marrow microenvironment and peripheral blood of myeloma patients and disease progression. J. Mol. Diagn. *17*, 669–678.
20. Indersie, E., Lesjean, S., Hooks, K.B., Sagliocco, F., Ernault, T., Cairo, S., Merched-Sauvage, M., Rullier, A., Le Bail, B., Taque, S., et al. (2017). MicroRNA therapy inhibits hepatoblastoma growth *in vivo* by targeting β-catenin and Wnt signaling. Hepatol. Commun. *1*, 168–183.
21. Wu, K., Yang, Y., Zhao, J., and Zhao, S. (2016). BAG3-mediated miRNA let-7g and let-7i inhibit proliferation and enhance apoptosis of human esophageal carcinoma cells by targeting the drug transporter ABCC10. Cancer Lett. *371*, 125–133.
22. Xie, L., Pelz, C., Wang, W., Bashar, A., Varlamova, O., Shadle, S., and Impey, S. (2011). KDM5B regulates embryonic stem cell self-renewal and represses cryptic intragenic transcription. EMBO J. *30*, 1473–1484.
23. Jia, Y., Yang, Y., Zhan, Q., Brock, M.V., Zheng, X., Yu, Y., Herman, J.G., and Guo, M. (2012). Inhibition of SOX17 by microRNA 141 and methylation activates the WNT signaling pathway in esophageal cancer. J. Mol. Diagn. *14*, 577–585.
24. Wang, X., Li, X., Wang, T., Wu, S.P., Jeong, J.W., Kim, T.H., Young, S.L., Lessey, B.A., Lanz, R.B., Lydon, J.P., and DeMayo, F.J. (2018). SOX17 regulates uterine epithelial-stromal cross-talk acting via a distal enhancer upstream of Ihh. Nat. Commun. *9*, 4421.
25. Matsumoto, S., Yamamichi, T., Shinzawa, K., Kasahara, Y., Nojima, S., Kodama, T., Obika, S., Takehara, T., Morii, E., Okuyama, H., and Kikuchi, A. (2019). GREB1 induced by Wnt signaling promotes development of hepatoblastoma by suppressing TGFβ signaling. Nat. Commun. *10*, 3882.
26. Hodgkinson, K., Forrest, L.A., Vuong, N., Garson, K., Djordjevic, B., and Vanderhyden, B.C. (2018). GREB1 is an estrogen receptor-regulated tumour promoter that is frequently expressed in ovarian cancer. Oncogene *37*, 5873–5886.

27. Shi, Y., Duan, Z., Zhang, X., Zhang, X., Wang, G., and Li, F. (2019). Down-regulation of the let-7i facilitates gastric cancer invasion and metastasis by targeting COL1A1. Protein Cell *10*, 143–148.

28. Song, J., Wang, L., Ma, Q., Yang, Y., Yang, Z., Wang, B., and He, N. (2018). Let-7i-5p inhibits the proliferation and metastasis of colon cancer cells by targeting kallikrein-related peptidase 6. Oncol. Rep. *40*, 1459–1466.

29. Raychaudhury, P., and Marians, K.J. (2019). The recombination mediator proteins RecFOR maintain RecA* levels for maximal DNA polymerase V Mut activity. J. Biol. Chem. *294*, 852–860.

30. Shen, X., Zhuang, Z., Zhang, Y., Chen, Z., Shen, L., Pu, W., Chen, L., and Xu, Z. (2015). JARID1B modulates lung cancer cell proliferation and invasion by regulating p53 expression. Tumour Biol. *36*, 7133–7142.

31. Kaypee, S., Sahadevan, S.A., Patil, S., Ghosh, P., Roy, N.S., Roy, S., and Kundu, T.K. (2018). Mutant and Wild-Type Tumor Suppressor p53 Induces p300 Autoacetylation. iScience *4*, 260–272.

32. Shigekawa, Y., Hayami, S., Ueno, M., Miyamoto, A., Suzaki, N., Kawai, M., Hirono, S., Okada, K.I., Hamamoto, R., and Yamaue, H. (2018). Overexpression of KDM5B/JARID1B is associated with poor prognosis in hepatocellular carcinoma. Oncotarget *9*, 34320–34335.

33. Xu, W., Zhou, B., Zhao, X., Zhu, L., Xu, J., Jiang, Z., Chen, D., Wei, Q., Han, M., Feng, L., et al. (2018). KDM5B demethylates H3K4 to recruit XRCC1 and promote chemoresistance. Int. J. Biol. Sci. *14*, 1122–1132.

34. Wang, Z., Tang, F., Qi, G., Yuan, S., Zhang, G., Tang, B., and He, S. (2014). KDM5B is overexpressed in gastric cancer and is required for gastric cancer cell proliferation and metastasis. Am. J. Cancer Res. *5*, 87–100.

35. Du, Y.C., Oshima, H., Oguma, K., Kitamura, T., Itadani, H., Fujimura, T., Piao, Y.S., Yoshimoto, T., Minamoto, T., Kotani, H., et al. (2009). Induction and down-regulation of Sox17 and its possible roles during the course of gastrointestinal tumorigenesis. Gastroenterology *137*, 1346–1357.

36. Ye, Y.W., Wu, J.H., Wang, C.M., Zhou, Y., Du, C.Y., Zheng, B.Q., Cao, X., Zhou, X.Y., Sun, M.H., and Shi, Y.Q. (2011). Sox17 regulates proliferation and cell cycle during gastric cancer progression. Cancer Lett. *307*, 124–131.

37. Chen, K., Fan, J., Luo, Z.F., Yang, Y., Xin, W.J., and Liu, C.C. (2018). Reduction of SIRT1 epigenetically upregulates NALP1 expression and contributes to neuropathic pain induced by chemotherapeutic drug bortezomib. J. Neuroinflammation *15*, 292.

38. Pasquier, M., and Hugli, O. (2019). Reply to: Low incidence of avalanche victims in cardiac arrest calls for multi-centre studies and registries for the validation of resuscitation guidelines. Resuscitation *144*, 197–198.

39. Laviolette, L.A., Hodgkinson, K.M., Minhas, N., Perez-Iratxeta, C., and Vanderhyden, B.C. (2014). 17β-estradiol upregulates GREB1 and accelerates ovarian tumor progression in vivo. Int. J. Cancer *135*, 1072–1084.

40. Cheng, R., Chen, Y., Zhou, H., Wang, B., Du, Q., and Chen, Y. (2018). B7-H3 expression and its correlation with clinicopathologic features, angiogenesis, and prognosis in intrahepatic cholangiocarcinoma. APMIS *126*, 396–402.

41. Ning, H., Albersen, M., Lin, G., Lue, T.F., and Lin, C.S. (2013). Effects of EdU labeling on mesenchymal stem cells. Cytotherapy *15*, 57–63.

42. Ma, H.L., Yu, S.J., Chen, J., Ding, X.F., Chen, G., Liang, Y., and Pan, J.L. (2020). CA8 promotes RCC proliferation and migration though its expression level is lower in tumor compared to adjacent normal tissue. Biomed. Pharmacother. *121*, 109578.

43. Wu, Q., and Yi, X. (2018). Down-regulation of long noncoding RNA MALAT1 protects hippocampal neurons against excessive autophagy and apoptosis via the PI3K/Akt signaling pathway in rats with epilepsy. J. Mol. Neurosci. *65*, 234–245.